www.revistageintec.net
ISSN: 2237-0722
revista GEINTEC
Gestão, Inovação e Tecnologias

Performance Analysis of Closed Loop Operation of BLDC Motor

CH.N. Narasimharao[1]; G. Durga Sukumar[2]; Y. Sinivasarao[3]
[1]Assistant Professor, Department of EEE, VFSTR University, India.
[1]cherukuri.narsi@gmail.com
[2]Professor, Department of EEE, Vignan Institute of Science and Technology, India.
[2]durgasukumar@gmail.com
[3]Assistant Professor, Department of EEE, VFSTR University, India.
[3]cnuiitr@gmail.com

Abstract
Industrial applications requires the minimized torque ripple along with the motor stable operation. The Hysteresis and pulse width modulation methods are used to obtain improved performance of BLDC motor. The torque ripples, speed control and the stability of BLDC motor were observed. The proposed system is mainly focused on the parameters such as motor speed; Stator current and Back EMF are to increase the performance level. The MATLAB/SIMULINK models of closed loop and dynamic modeling for stability are also presented.

Key-words: BLDC Motor, Hysteresis & PWM Models, Stability Analysis.

1. Introduction

BLDC motor is the best choice for different power level applications, because of its merits such as high efficiency, different level of speed control, high torque-inertia ratio and low electromagnetic interference. The noise level of BLDC motor is quite low. Stator consists of three phase windings arrangements are based on trapezoidal in nature[1]-[2]. The permanent magnet rotor acts as a field, so there is no need of mechanical commutator and brush arrangement. Electronic commutator with hall sensor arrangement is introduced to get accurate control of rotor position from feedback signal[3]. So the limitations due to mechanical commutator with brush arrangement are overcome with the help of semiconductor technology and intelligent controllers[4]. When compare to other special machines BLDC has twenty percentage high power densities because of its low torque ripples from trapezoidal back EMF[5].

BLDC motor is modelled using with gate drive inverter and back-EMF generation circuit, BLDC motor with 60^0 phase angle for three phases as 360^0. The motor is operated with corresponding terminal voltage, resistance, inductance, torque and EMF constant[6]-[7]. The poles of rotor crossing near the hall sensor, that will give high or low signal indicating by N and S poles. The hall sensor are placed exactly 120 electrical degrees apart from each other. The rotor position estimation is achieved by three hall sensors which are placed 120 electrical degrees apart from each other[8]-[9]. The stable operation of BLDC motor is to maintained in industrial applications. The stable operation includes noise less operation, reduced ripples in torque and speed [10].

Modeling of BLDC Motor

Where three phase voltages in stator are $V_{ry,}$ V_{yb} and, V_{br}; R is the per phase stator resistance; the stator phase currents are i_r,i_y and i_b ; per phase inductance is L; Let assume it's a balanced three phase system i.e, resistance in all the phases are equal.

$$v_{ry} = R(i_r - i_y) + L\frac{d}{dt}(i_r - i_y) + e_r - e_y \tag{1}$$

$$v_{yb} = R(i_y - i_b) + L\frac{d}{dt}(i_y - i_b) + e_y - e_b \tag{2}$$

$$v_{br} = R(i_b - i_r) + L\frac{d}{dt}(i_b - i_r) + e_b - e_r \tag{3}$$

$$F(\theta_e) = \begin{cases} 1, & 0 \leq \theta_e \leq 120 \\ 1 - \frac{6}{180}(\theta_e - 120) & 120 \leq \theta_e < 180 \\ -1 & 180 \leq \theta_e < 240 \\ -1 + \frac{6}{180} & 240 \leq \theta_e < 360 \end{cases} \tag{4}$$

The phase EMF, current and electromagnetic torque equations are represented below.

$$e_r = \frac{k_e}{2}\omega_m F\theta_e \tag{5}$$

$$e_y = \frac{k_e}{2}\omega_m F(\theta_e - 120) \tag{6}$$

$$e_b = \frac{k_e}{2}\omega_m F(\theta_e - 240) \tag{7}$$

The balancing of stator current is difficult, which is given as

$$I_a + I_b + I_c = 0 \tag{8}$$

$$T_e = \frac{k_t}{2}\left[F(\theta_e)i_r + F(\theta_e - 120)i_y + F(\theta_e - 240)i_b\right] \tag{9}$$

$$T_e = k_f\omega_m + J\frac{d\omega_m}{dt} + T_L \tag{10}$$

Closed Loop Operation of Brushless DC Motor

The error in the speed (difference of reference and actual) is given to PI controller which produced the reference current. The three reference currents and actual currents are given to hysteresis or PWM controller which gives the pulses for the inverter to supply the brushless dc motor shown in fig 1.

Fig. 1 - Block Diagram of Control Scheme of BLDC Motor Drive

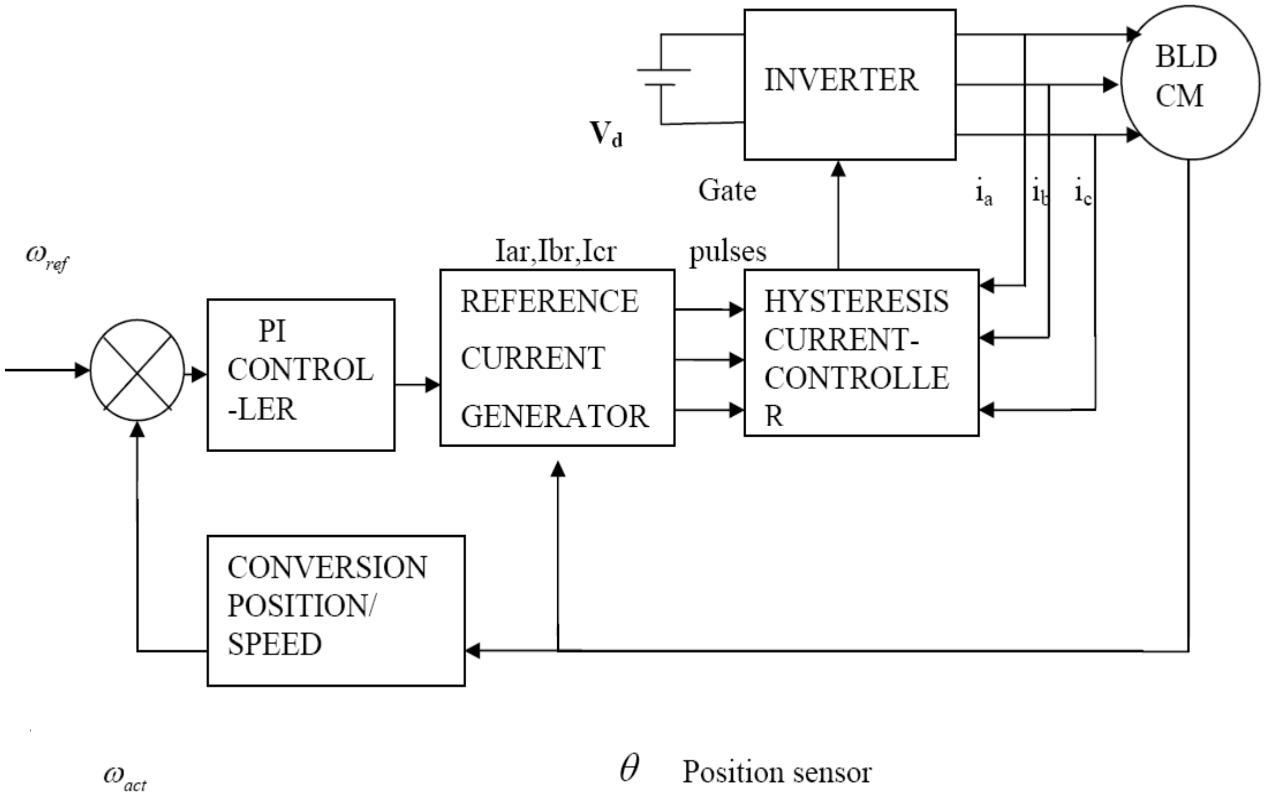

Inverter

The inverter shown in error coming from hysteresis controller. The table1 shows relation between rotor position and three phase voltages.

Table 1 - Inverter Voltages with Rotor Position

Theta	Switches ON	Van	Vbn	Vcn
0^0-60^0	S1 and S6	Vd/2	-Vd/2	0
60^0-120^0	S1and S2	Vd/2	0	-Vd/2
120^0-180^0	S2 and S3	0	Vd/2	-Vd/2
180^0-240^0	S3 and S4	-Vd/2	Vd/2	0
240^0-300^0	S4 and S5	-Vd/2	0	Vd/2
300^0-360^0	S5 and S6	0	-Vd/2	Vd/2

In the 120 degree conduction mode each thyristor conducted for 120 degree. Whereas the in 180 degree conduction mode, conduction angle for each thyristor is 180 degree. In the 180 there may be a chance of getting short of phase, this can be overcome in 120 degree mode. For every 60 degree interval only two switches are in ON position in 120 degree mode, where as in 180 degree mode three switches are in ON position.

Proportional-Integral Controller

Transfer function of PI controller is $\frac{O(s)}{E(s)} = Kp + \frac{Ki}{s}$ (11)

Where O(s) is the output of PI controller and E(s) error input for the PI controller.

Hysteresis Controller

Hysteresis current controller is shown in fig 2.

Fig. 2 - Hysteresis Controller

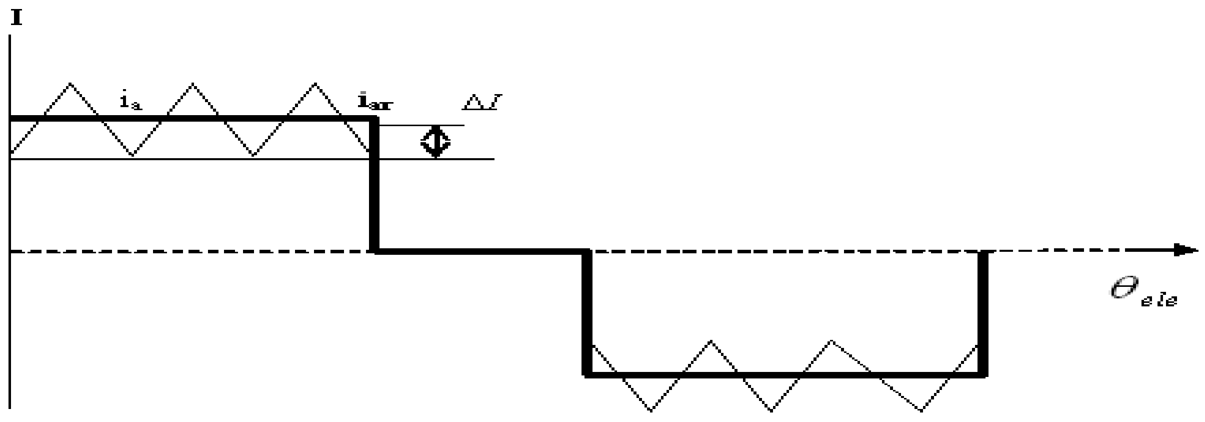

Table 2 - Relation between the Error and Switches

Error (Δ I = i_{ar} - i_a)	**Switches**	**Voltage**
$(i_{ar}-i_a) > \Delta I$	T_1 ON T_4 OFF	Van=Vd/2
$(i_{ar}-i_a) < -\Delta I$	T_1 OFF T_4 ON	Van= -Vd/2
$(i_{br}-i_b) > \Delta I$	T_3 ON T_6 OFF	Vbn=Vd/2
$(i_{br}-i_b) < -\Delta I$	T_3 OFF T_6 ON	Vbn= -Vd/2
$(i_{cr}-i_c) > \Delta I$	T_5 ON T_2 OFF	Vcn=Vd/2
$(i_{cr}-i_c) < -\Delta I$	T_5 OFF T_2 ON	Vcn= -Vd/2

In the simplest form of hysteresis current control, a fixed hysteresis band is used around on the reference current. It is set to ensure that the maximum acceptable switching losses not exceeded under any operating conditions of the drive.

Current Reference Block

$$T_e^* = H*(f_a(\theta)*i_{ar} + f_b(\theta)*i_{br} + f_c(\theta)*i_{cr}) \quad (12)$$

Due the result of sign relationship, the reference torque magnitude can be written as

$$T_e^* = 2*H*I_p^* \quad (13)$$

Assume reference current magnitude $Ip^* = I_s$

From the equation (13) $I_s = \frac{T_e^*}{2*H}$ (14)

The relation between the rotor position and three phase reference currents is shown in the table 3.

Table 3 - Relationship between Reference Current and Rotor Position

θ_{ele}	**I_{ar}**	**I_{br}**	**I_{cr}**
0^0-60^0	0	I_s	- I_s
60^0-120^0	I_s	0	- I_s
120^0-180^0	I_s	- I_s	0
180^0-240^0	0	- I_s	I_s
240^0-300^0	- I_s	0	I_s
300^0-360^0	- I_s	I_s	0

ISSN: 2237-0722
Vol. 11 No. 4 (2021)
Received: 17.07.2021 – Accepted: 16.08.2021

2. Stability Analysis

Dynamic Modeling of BLDCM

During two phase conduction, the entire dc voltage is applied to the two phases and the transfer function for the stator current is given by

$$\frac{I_a(s)}{V_d(s)-E(s)}=\frac{K_a}{1+sT_a}\text{, Where } K_a=\frac{1}{R_a}=\frac{1}{2*R_s}\text{ (since } R_a=2*R_s\text{) and } T_a=\frac{2*(L-M)}{2*R_s}$$

R_s= stator resistance per phase, L= self-inductance per phase, M= mutual inductance per phase

The electromagnetic torque is given by $T_e=K_b*I_a$

As we know that $J\frac{d\omega_m}{dt}+B_1*\omega_m=T_e-T_l$

Where B_1 is the friction coefficient of the motor and J is inertia of the machine

Assume that load is proportional to speed

$$T_l=T_{L0}+B_2*\omega_m \text{ \& } \frac{\omega_m(s)}{T_e(s)}=\frac{\frac{1}{B_t}}{1+sT_m}\text{, Where } T_m=\frac{J}{B_t}\text{ (motor time constant) } B_t=B_1+B_2$$

From the above equations, the BLDC motor can be modelled as shown in fig 3.

Fig. 3 - Equivalent Model of BLDC Motor

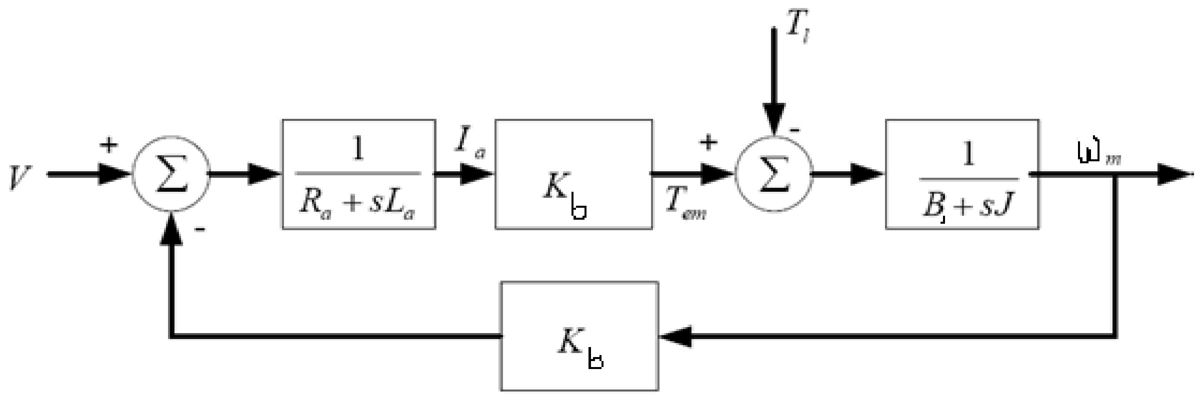

From the power converter $\frac{V_a(s)}{V_c(s)}=\frac{K_r}{1+sT_r}$

Current and speed feedbacks have a low pass filters with transfer functions given by

ISSN: 2237-0722
Vol. 11 No. 4 (2021)
Received: 17.07.2021 – Accepted: 16.08.2021

$$H_c = \frac{K_c}{T_c s + 1} \ \& \ H_w = \frac{K_w}{T_w s + 1}$$

Fig. 4 - BLDM Motor Control Diagram with Inner Loop Current Controller

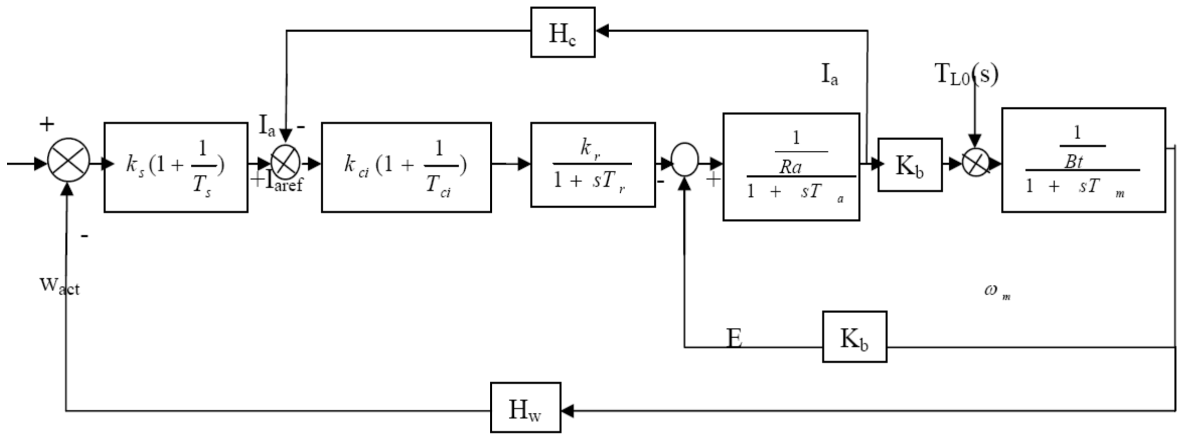

$E = K_b * \omega_m$, where $K_b = 2 * H$ ($H = B * l * r * N$)

The modified block diagram of BLDC motor shown in fig.

Fig. 5 - Final Speed Control Diagram of BLDC Motor with Inner Loop Current Controller

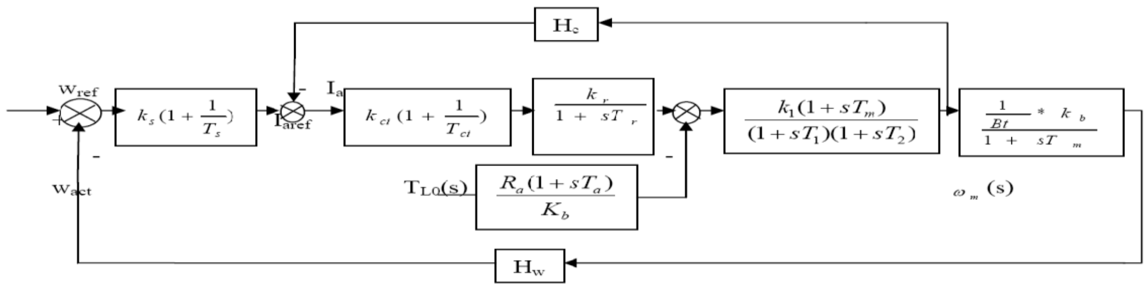

Where $K_1 = \frac{B_t}{B_t * R_a + K_b{}^2}$ and $T_1 + T_2 = \frac{(T_a + T_m) * B_t * R_a}{B_t * R_a + K_b{}^2}$

$T_1 * T_2 = \frac{T_m * T_a * B_t * R_a}{B_t * R_a + K_b{}^2}$ (Where T_m, T_1, T_2 are the motor time constants)

3. Simulation of BLDCM Using MATLAB/Simulink

BLDCM Simulink Modeling

The modelled BLDC motor block diagram using Simulink as shown in Fig 6.

Fig. 6 - Simulink Diagram of BLDC Motor Modelling

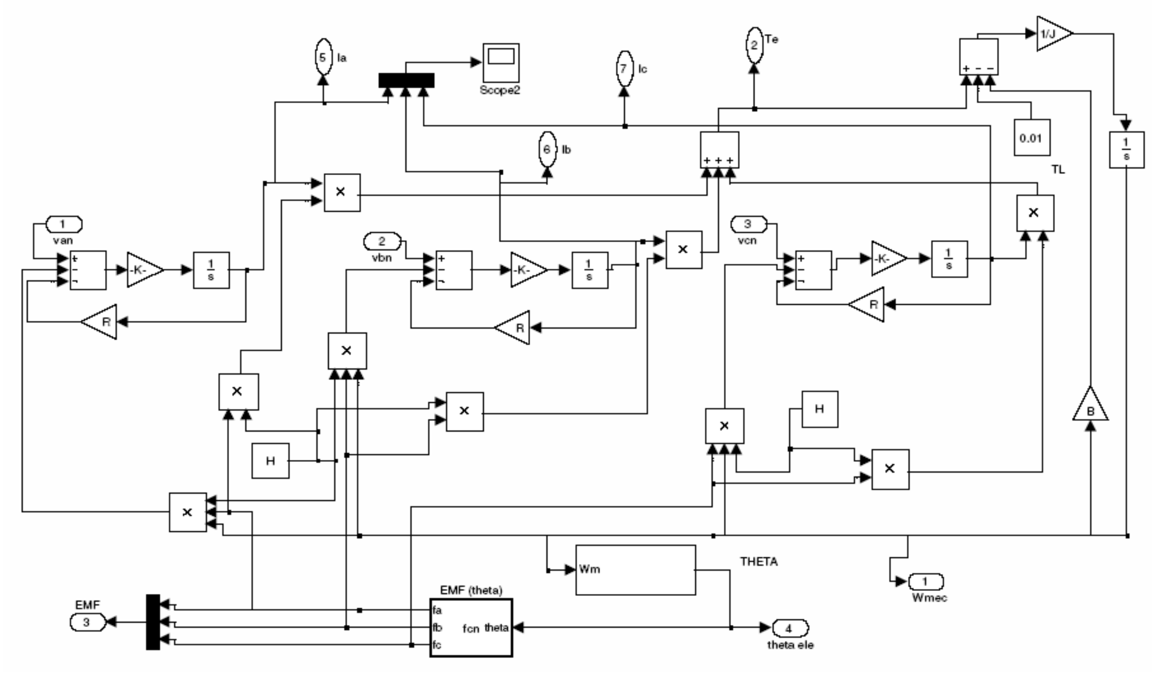

Brushless DC Motor with Hysteresis Current Controller

The hysteresis controller compares reference and actual currents to limit the actual current in the pre-defined band, which generates the pulses for the inverter.

Fig. 7 - Simulink Diagram of BLDC Motor with Hysteresis Controller

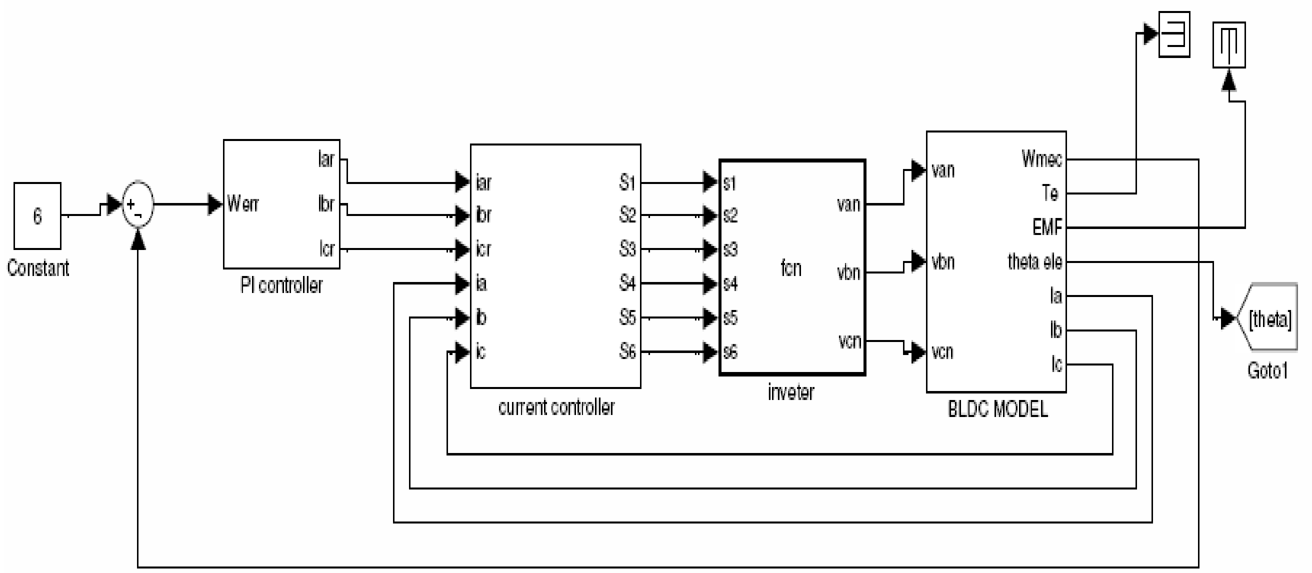

Hysteresis Controller Simulink Model

Fig. 8 - Simulink Diagram of Hysteresis Controller

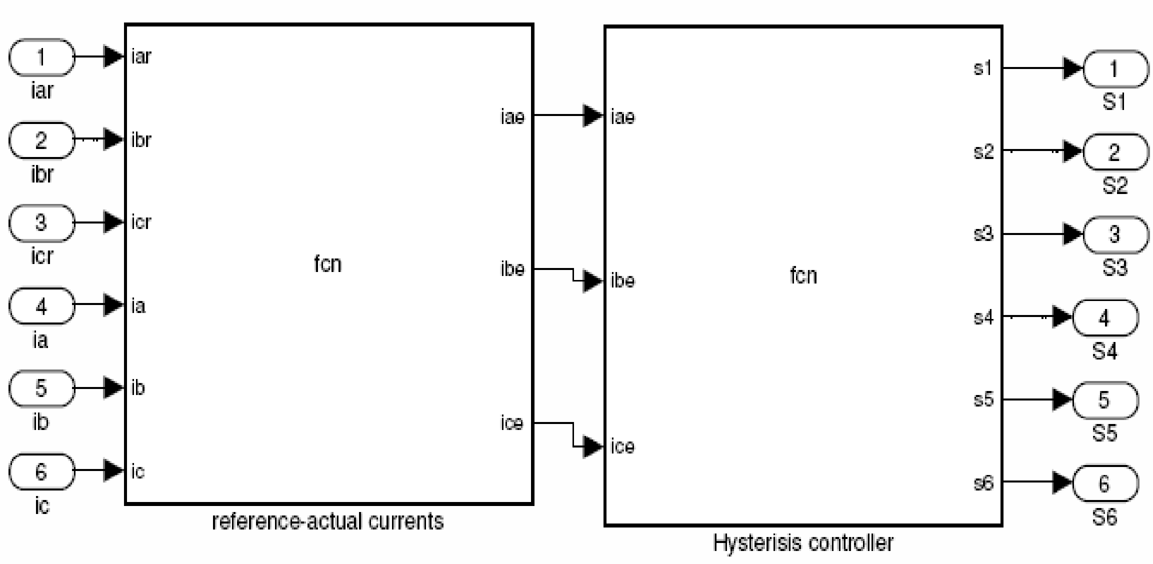

PI Controller and Reference Current Generation

Fig.9: shows the Simulink diagram of PI controller and reference current generation.

Fig. 9 - Simulink Diagram of PI Controller and Reference Current Generation

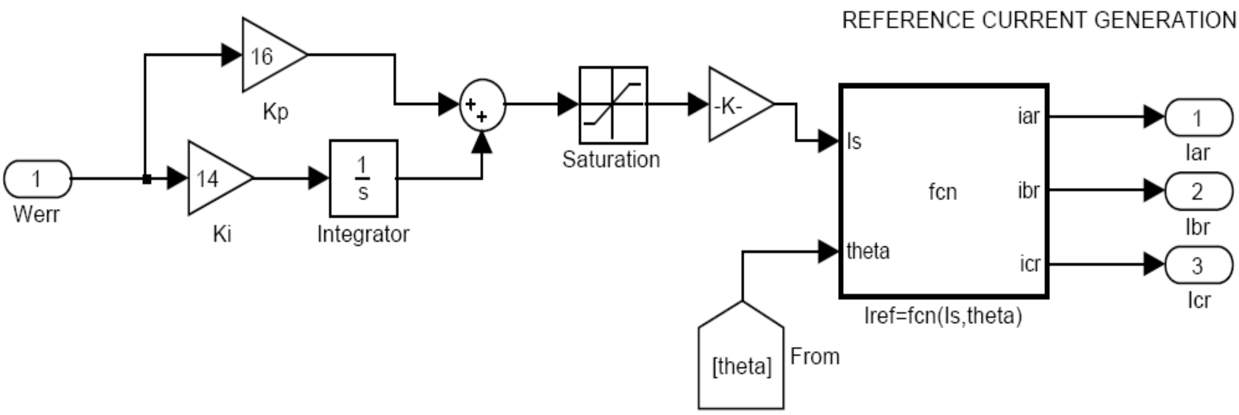

PWM Current Controller

Comparing the repeating sequence with the current error (difference between the reference and actual), according to that inverter operates and supplies the BLDC motor.

Fig. 10 - Simulink Diagram of PWM Controller

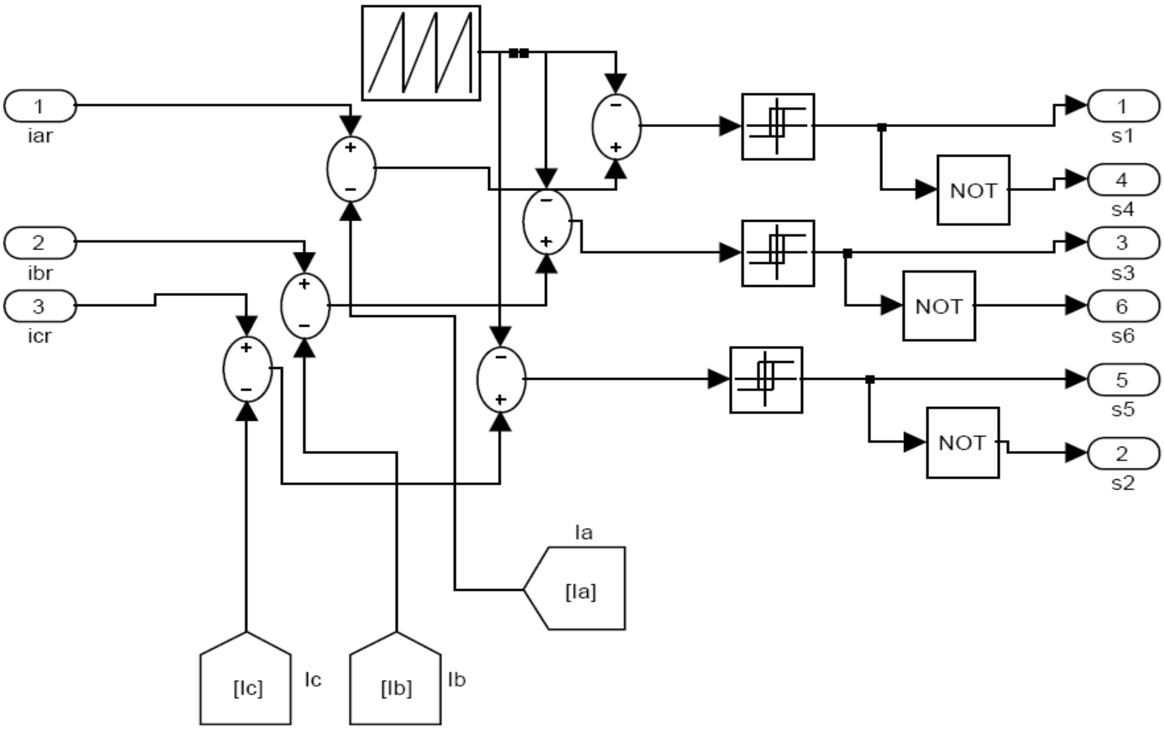

Simulink Diagram of Speed Control of BLDC Motor for Stability Analysis

The speed of BLDC motor can be controlled with inner loop current controller. In this Simulink model we have given a step input and observed that the output follows input.

Fig. 11 - Simulink Diagram of Dynamic Modeling of BLDC Motor

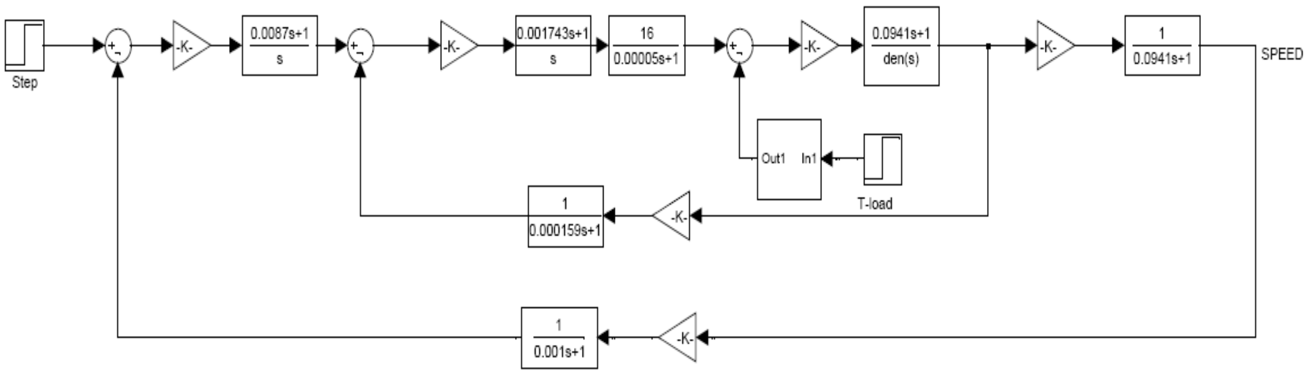

ISSN: 2237-0722
Vol. 11 No. 4 (2021)
Received: 17.07.2021 – Accepted: 16.08.2021

Simulation Results and Discussions

Fig. 12 - Rotor Position of the BLDC Motor

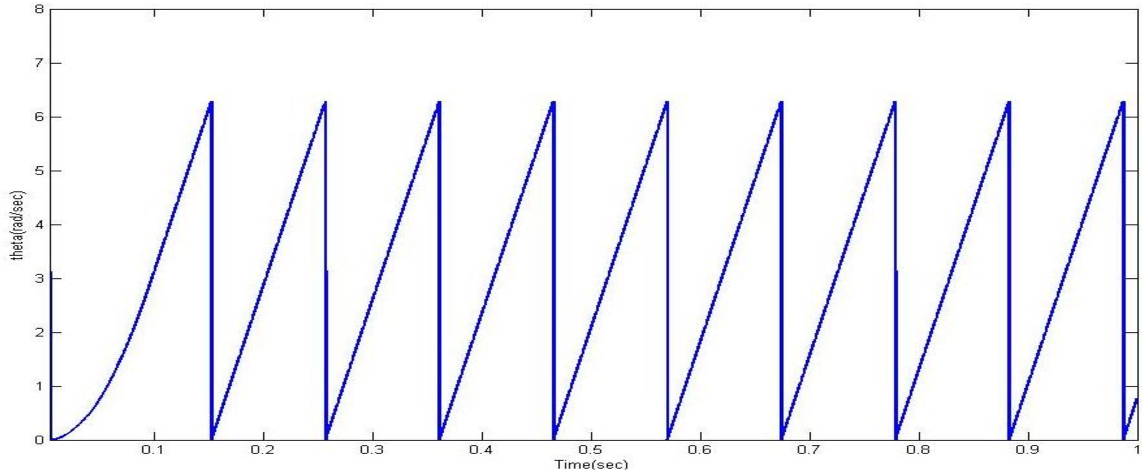

Fig. 13 - Back EMF of the BLDC Motor for One Cycle

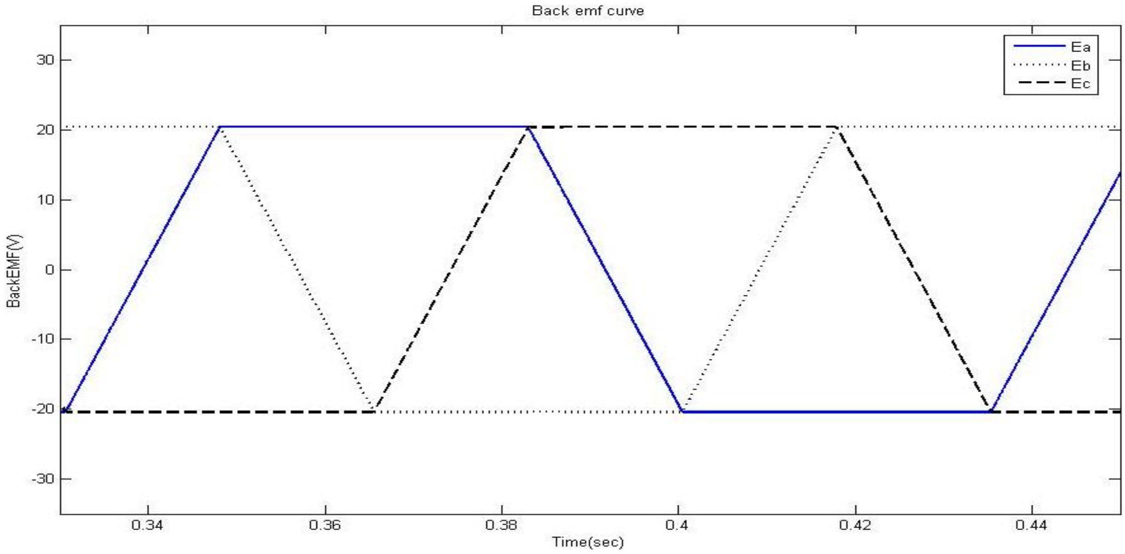

Fig. 14 - Speed of the BLDC Motor with Controller

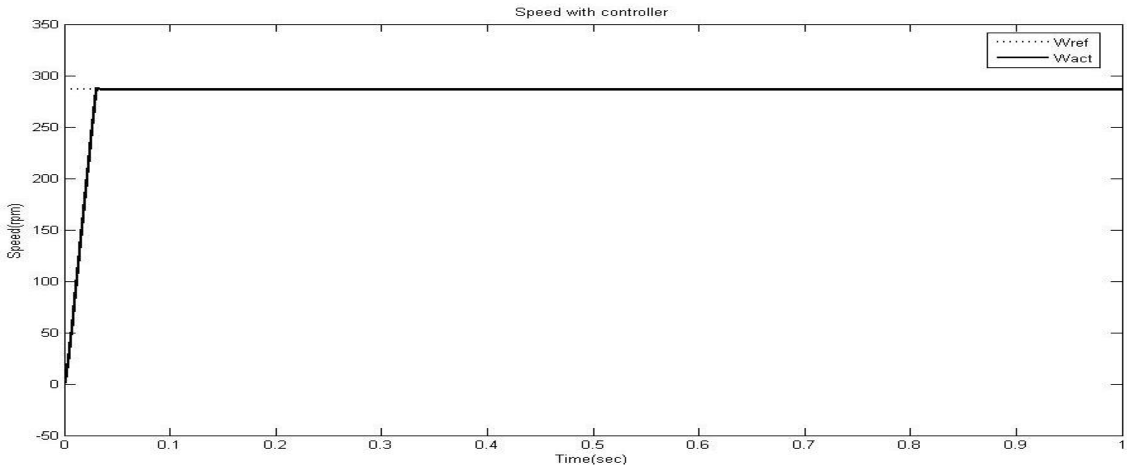

ISSN: 2237-0722
Vol. 11 No. 4 (2021)
Received: 17.07.2021 – Accepted: 16.08.2021

Fig. 15 - Electromagnetic Torque of the BLDC Motor with Hysteresis Controller in Steady State

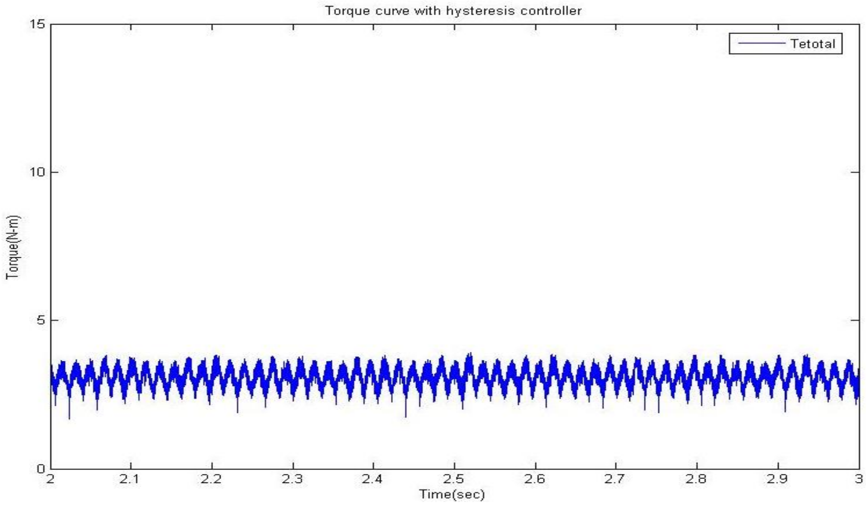

Fig. 16 - Electromagnetic Torque of BLDC Motor with PWM Controller in Steady State

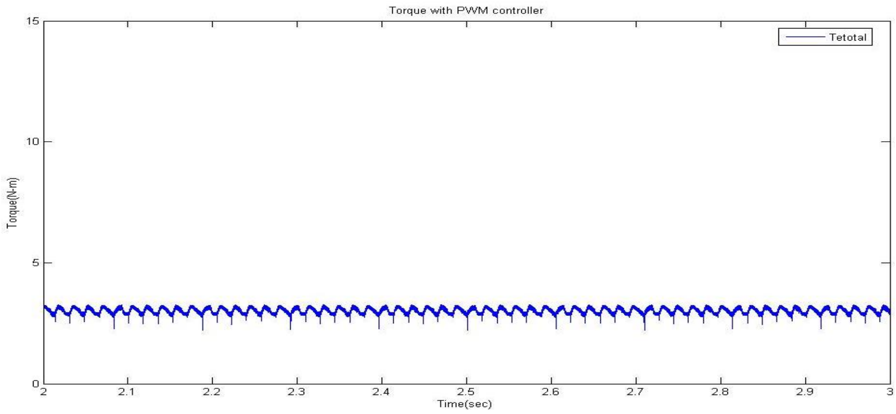

Stability Curves

In simulation fig.17 output follows the input.

Fig. 17 - Step Response of BLDC Motor Under Without Load

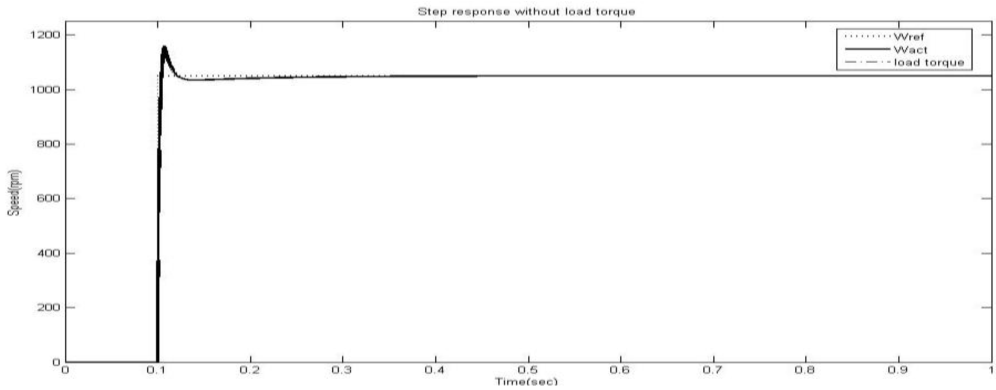

In simulation fig.18 when sudden load applied, output follows the input.

Fig. 18 - Step Response of BLDC Motor with Load at 0.5 Sec

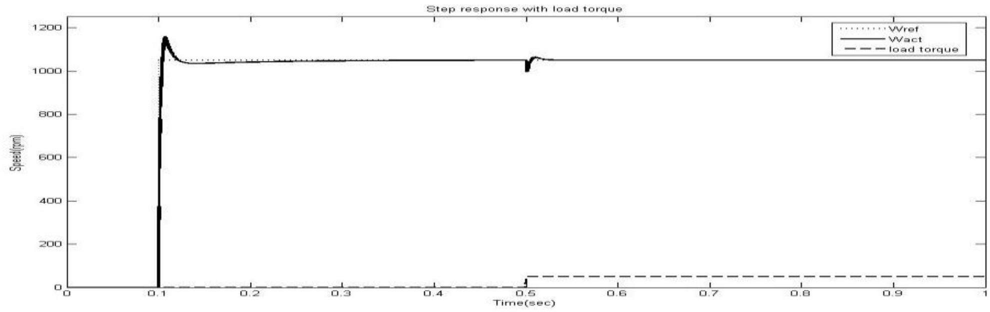

In simulation fig.19 all poles are in the left half of s-plane, so our system is stable.

Fig. 19 - Root Locus Diagram for BLDC Motor

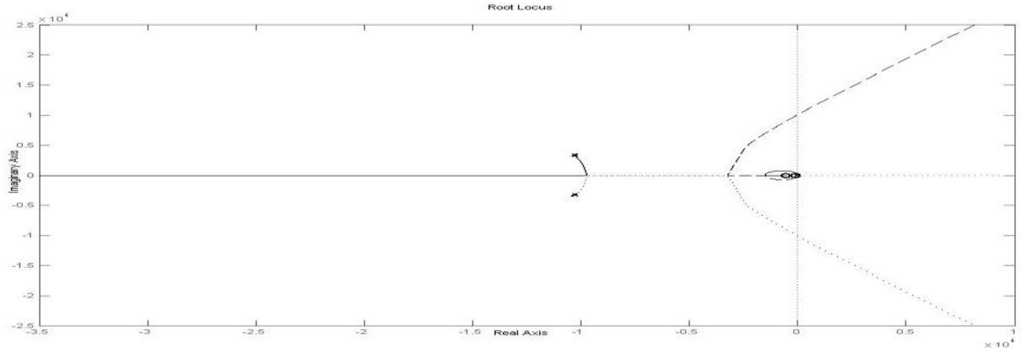

4. Conclusions

The Simulink models of closed loop operation of BLDC motor with PWM, hysteresis controller, stability block diagram obtained. With the help of inverter voltage with respect to rotor position, operation of brushless DC motor using controller is obtained. The final outer speed control block diagram of brushless DC motor with inner loop current controller is obtained. The simulation results of brushless DC motor using hysteresis controller & PWM controller, step response of speed without load and with load and the Stability analysis of BLDC motor were obtained. The Motor performance was observed with the waveforms of reduced torque ripples, speed controlled and the stability of BLDC motor.

References

R. Krishnan, A text book of *Electrical motor drives modeling, analysis, and control.*

H.T. Wang; Z.J. Liu; S.X. Chen; J.P. Yang "Application of Taguchi method to robust design of BLDC motor performance" *IEEE Transactions on Magnetics,* Year: 1999 | Volume: 35, Issue: 5.

In-Soung Jung; Ha-Gyeong Sung; Yon-Do Chun; Jin-Hwan Borm "Magnetization modeling of a bonded magnet for performance calculation of inner-rotor type BLDC motor" *IEEE Transactions on Magnetics,* Year: 2001, Volume: 37, Issue: 4.

Mohamed Z. Youssef "Design and Performance of a Cost-Effective BLDC Drive for Water Pump Application", *IEEE Transactions on Industrial Electronics,* Year: 2015, Volume: 62, Issue: 5.

Xinda Song; Bangcheng Han; Kun Wang "Sensorless Drive of High-Speed BLDC Motors Based on Virtual Third-Harmonic Back EMF and High-Precision Compensation" *IEEE Transactions on Power Electronics,* Year: 2019, Volume: 34, Issue: 9.

Woongkul Lee; Ju Hyung Kim; Wooyoung Choi; Bulent Sarlioglu "Torque Ripple Minimization Control Technique of High-Speed Single-Phase Brushless DC Motor for Electric Turbocharger" *IEEE Transactions on Vehicular Technology,* Year: 2018, Volume: 67, Issue: 11.

Geun-Ho Lee; Sung-Il Kim; Jung-Pyo Hong; Ji-Hyung Bahn "Torque Ripple Reduction of Interior Permanent Magnet Synchronous Motor Using Harmonic Injected Current", *IEEE Transactions on Magnetics,* Year: 2008, Volume: 44, Issue: 6.

Yong-Kai Lin; Yen-Shin Lai "Pulse width Modulation Technique for BLDCM Drives to Reduce Commutation Torque Ripple Without Calculation of Commutation Time". *IEEE Transactions on Industry Applications,* Year: 2011, Volume: 47, Issue: 4.

Dae-kyong Kim; Kwang-woon Lee; Byung-il Kwon "Commutation Torque Ripple Reduction in a Position Sensorless Brushless DC Motor Drive", *IEEE Transactions on Power Electronics,* Year: 2006, Volume: 21, Issue: 6.

Tuanjie Li;Jiaxing Zhou "High-Stability Position-Sensorless Control Method for Brushless DC Motors at Low Speed", *IEEE Transactions on Power Electronics,* Year: 2019, Volume: 34, Issue: 5.